

Liquid-crystalline ordering in rod–coil diblock copolymers studied by mesoscale simulations

BY A. ALSUNAIDI¹, W. K. DEN OTTER² AND J. H. R. CLARKE³

¹*Department of Physics, King Fahd University of Petroleum and Minerals, Dhahran 31261, Saudi Arabia (asunaidi@kfupm.edu.sa)*

²*Faculty of Science and Technology, University of Twente, PO Box 217, 7500 AE Enschede, The Netherlands (w.k.denotter@utwente.nl)*

³*Department of Chemistry, UMIST, PO Box 88, Manchester M60 1QD, UK (jhrc@umist.ac.uk)*

Published online 3 June 2004

Using mesoscale dissipative particle dynamics (DPD) simulations, which ignore all atomistic details, we show the formation of lamella mesophases by cooling a fully disordered system composed of symmetric (A₇B₇) rod–coil diblock copolymers. Equilibration is achieved very rapidly using DPD, and isotropic, smectic A and crystalline phases of the rod-like blocks can be observed either by heating or cooling. An interesting pseudo-smectic phase can be characterized when the order–disorder transition temperature is above the clearing temperature. This phase gradually fades into a normal microphase-separated structure as the system is heated through the clearing temperature. Simulations of pure rods, however, show the formation of isotropic, nematic, smectic A and crystalline phases.

Keywords: rod–coil copolymer; liquid crystal; mesoscale simulation; dissipative particle dynamics

1. Introduction

Microphase ordering in block copolymers and mesophase formation in thermotropic liquid crystals are two examples of phenomena that manifest themselves primarily on mesoscopic length- and time-scales. Both processes occur in a large class of liquid-crystal molecules and polymers of practical interest where flexible tails are attached to one or more rigid blocks (Kelker & Hatz 1980). There have been several recent experimental (Chen *et al.* 1996; Jenekhe & Chen 1998, 1999; Lee *et al.* 2001) and theoretical (Duchs & Sullivan 2000; Matsen & Barrett 1998; Reenders & ten Brinke 2002; Semenov 1991; Semenov & Vasilenko 1986) studies aimed at understanding the interplay between microphase ordering and mesophase transitions.

Fifty years ago, Onsager (1949) showed that long rod-like particles, interacting only through excluded-volume interactions, form a nematic phase upon increasing the density. Since then, many computer simulations of liquid-crystal behaviour have been performed using hard-core models, such as spherocylinders and the Gay–Berne

One contribution of 21 to a Theme ‘Connecting scales: micro, meso and macro processes’.

potential. These simple models already display many of the interesting and complicated properties of liquid crystals. More recently, simulations have been extended to rod–coil systems (Affouard *et al.* 1996; McBride *et al.* 2001; Nicklas *et al.* 1994; van Duijneveldt *et al.* 2000), again using hard-core potentials. Of particular interest are studies of the effect of the coil–block structure on the stabilization of certain liquid-crystalline phases. Affouard *et al.* (1996), for example, carried out molecular dynamics simulations for a system composed of multi-bead semi-flexible chains where the beads are connected by anharmonic springs and the chains interact by the Lennard-Jones potential. They only observed solid, smectic A and isotropic liquid phases, while the nematic phase was not observed. van Duijneveldt *et al.* (2000) studied a model of hard spherocylinders with a length-to-width ratio of 5, attached to a flexible tail of 5 units. In their *NPT* (constant pressure) Monte Carlo simulation, they observed smectic A and crystal phases, in addition to the isotropic phase. Again, their model does not appear to have a stable nematic phase. Similar observations of the stabilization of the smectic phase and the suppression of the nematic phase due to the attachment of a flexible tail were reported by McBride *et al.* (2001).

In this work, we study phase ordering of rods in lamellae formed by the microphase separation of symmetric A_7B_7 rod–coil diblock copolymers. For this, we performed mesoscale simulations of rod–coil block copolymers using dissipative particle dynamics (DPD); this is a particle-based simulation technique in which particles interact via soft potentials and is well suited to the study of mesoscale phenomena. It was recently used by Groot & Madden (1998) to study mesophase formation of coil–coil diblock copolymers in the *NVT* ensemble. They found that lamellar, perforated lamellar, hexagonal and micellar phases were produced, depending on the length ratio of both blocks. Their DPD gave a near-quantitative match with the theory (Bates & Fredrickson 1990) for the locations of phase transitions.

Although we have studied the rod–coil copolymer for different values of rod-to-coil ratios, this article will focus on the competition between microphase ordering and liquid-crystalline transitions in symmetric (rod-to-coil volume fraction $f = 0.5$) rod–coil diblock copolymers. More specifically, we would like to know how phase ordering is affected by attaching a tail to a rigid rod. This study is different from some of the previous theoretical models (Matsen & Barrett 1998; Semenov 1991; Semenov & Vasilenko 1986) in the fact that the high-temperature phase is the isotropic phase and not the nematic. Liquid-crystalline ordering occurs only after microphase separation, which enables us to study the nature of the transitions in such systems. In addition, we have made detailed comparisons with the related pure-rod system.

The organization of this paper is as follows: in the next section the DPD simulation method and the models studies will be described. The results of our simulation for the rod–coil copolymer, A_7B_7 , and the pure rod, A_7 , models will be presented in § 3. Finally, a conclusion is given in § 4.

2. Simulation method

The underlying idea behind DPD is that every particle represents a collection of atoms, just like the beads in a bead–spring model of a polymer. Because of this coarse-grained nature, the total force on particle i is a sum of three pairwise additive forces:

$$\mathbf{f}_i = \sum_{j \neq i} \mathbf{f}_{ij}^C + \sum_{j \neq i} \mathbf{f}_{ij}^D + \sum_{j \neq i} \mathbf{f}_{ij}^R, \quad (2.1)$$

where the sums run over all neighbouring particles j within a cut-off distance r_c . The first force is a conservative force,

$$\mathbf{f}_{ij}^C = a_{ij}\omega_C(r_{ij})\hat{\mathbf{r}}_{ij}, \quad (2.2)$$

where a_{ij} sets the strength, $\omega_C(r_{ij})$ gives the shape of the potential, and $r_{ij}\hat{\mathbf{r}}_{ij} = \mathbf{r}_i - \mathbf{r}_j$, with the hat denoting a unit vector. Traditionally, DPD particles interact via a soft repulsive potential of the form

$$\omega_C(r_{ij}) = 1 - |r_{ij}|/r_c. \quad (2.3)$$

Since a DPD particle represents a collection of many atoms, averaging over the internal degrees of freedom gives rise to a dissipative (or friction) force

$$\mathbf{f}_{ij}^D = -\gamma\omega_D(r_{ij})(\hat{\mathbf{r}}_{ij} \cdot \mathbf{v}_{ij})\hat{\mathbf{r}}_{ij}, \quad (2.4)$$

and a random (or stochastic) force

$$\mathbf{f}_{ij}^R = \sigma\omega_R(r_{ij})\theta_{ij}(t)\hat{\mathbf{r}}_{ij}. \quad (2.5)$$

Here, γ is the friction coefficient, σ controls the magnitude of the random force and ω_D and ω_R give the distance dependence of these two contributions. The random number $\theta_{ij}(t)$ has zero average, unit variance, differs for each particle pair, and varies in time without memory, i.e. $\langle\theta_{ij}(t)\theta_{kl}(t')\rangle = (\delta_{ik}\delta_{jl} + \delta_{il}\delta_{jk})\delta(t - t')$. In numerical simulations it is common practice to assume that the random force is constant over the entire time-step δt , in which case the friction force takes the form

$$\mathbf{f}_{ij}^R = \sigma\omega_R(r_{ij})\zeta_{ij}(t)\delta t^{-1/2}\hat{\mathbf{r}}_{ij}. \quad (2.6)$$

The new random variable $\zeta_{ij}(t)$ has zero mean, unit variance and is uncorrelated for each particle pair and each time-step. The balance between the random and the friction forces (which act, respectively, as heat source and heat sink) is provided by the condition that

$$\sigma^2\omega_R^2(r) = 2\gamma\omega_D(r)k_B T, \quad (2.7)$$

where k_B is the Boltzmann constant. We follow the usual choice of $\omega_D = \omega_R^2 = (1 - r/r_c)^2$. From this equation it is evident that the friction and random forces together act as a thermostat to the system.

Note that all forces, conservative as well as friction and random forces, are of the form $\mathbf{f}_{ij} = -\mathbf{f}_{ji}$ needed for proper hydrodynamics. For an overview of the DPD method, concentrating on its applications to polymers, we refer the reader to den Otter & Clarke (2004). It should be noted that these simulations of polymers, as well as the simulations discussed here, differ from the original DPD method in the interpretation of the particles. Rather than regarding a particle as a collection of solvent molecules, a particle is considered as a section of a larger molecule. The former approach can be applied to the current ordering phenomena only if the particles are equipped with extra coordinates describing their state of internal ordering, with the coupling between these coordinates and the overall flow field incorporated in their equations of motion. Fine-grained models, like the one considered here, might help establish such a model.

The dynamics of the DPD particles are followed by solving Newton's equation of motion, with the above forces, by means of the Verlet leapfrog algorithm (den Otter

& Clarke 2001). In the simulation we choose the mass of the particles $m = 1$ as the unit of mass and the cut-off radius $r_c = 1$ as the unit of distance. The conservative force constant, the temperature (henceforth we will use ‘temperature’ to refer to $k_B T$) and other energy-dependent quantities are expressed in units of energy. In particular, the unit of time is given by $t = r_c^{1/2} m T^{-1/2}$. We selected a time-step of $\delta t = 0.04$. At this value of the time-step, the inaccuracies in the integration of the friction and random forces lead to a kinetic temperature, $T_{\text{kin}} = 3m \langle \mathbf{v}_i^2 \rangle$, only moderately higher than the desired temperature (den Otter & Clarke 2001; Groot & Warren 1997).

In our simulations, the rods are modelled as seven fused spheres, each interacting according to equations (2.2) and (2.3). The distance between consecutive spheres is fixed at $\frac{2}{3}r_c$. From the location of the first peak in the radial distribution function at about $0.65r_c$ (in both ordered and disordered pure-rod systems), we deduce that the actual length-to-width ratio of our rods is about 4. During the simulation, a constraining routine is used to keep the spheres aligned and equidistant (Ciccotti *et al.* 1982). In short, the forces on the seven particles of a rod are converted into a net force on the two end particles, and the equations of motion for these two particles are solved, using the standard SHAKE routine to keep them at a fixed distance. The positions of the five intermediate particles are then readily calculated by a linear interpolation at the end of each time-step. The flexible coil is modelled as a chain of seven particles. Adjacent spheres are connected by harmonic springs, $\mathbf{f}_{ij}^S = C\mathbf{r}_{ij}$, with the spring constant $C = 2$ chosen such that the average bond length roughly coincides with the first peak in the radial distribution function of a monomer liquid (Groot & Warren 1997). This same criterion was also used to establish the distance between the particles in the rod.

Groot & Warren (1997) have shown the existence of a relationship between the repulsion parameter and the density in a polymeric system. In order to match the compressibility of water, for instance,

$$a_{ii}\rho = 75T, \quad (2.8)$$

where a_{ii} is the force constant between like particles. Since this study is done at a density of $\rho \approx 4$ to ensure a high number of neighbour interactions, the repulsion parameter was set at the usual value of $a_{ii} = 20$ (Groot & Warren 1997). The same authors also provided approximate relationships between the Flory–Huggins parameter χ and the repulsion parameter a_{ij} between unlike particles. For $\rho = 4$, we interpolated the equations provided for $\rho = 3$ and 5 to get

$$\Delta a = a_{ij} - a_{ii} \approx 2.05\chi T. \quad (2.9)$$

This result serves as a crude indication for the link between simulation results and experimental data.

Our simulations were carried out at constant pressure and temperature (NPT ensemble) using the Berendsen barostat (Allen & Tildesley 1987) and the DPD thermostat. To obtain any desired temperature, we opted to keep the friction constant at $\gamma = 2.66$, while varying σ . A constant-pressure routine allowed all box dimensions to change independently, minimizing the effect of the box’s size and shape on the final equilibrium structure. The diagonal elements of the pressure were fixed to 30, while setting the non-diagonal elements to zero. The initial box had dimensions $22 \times 22 \times 22$, with periodic boundary conditions applied in all directions. For the rod–coil copolymer system, we simulated 3000 copolymers each with 14 DPD particles

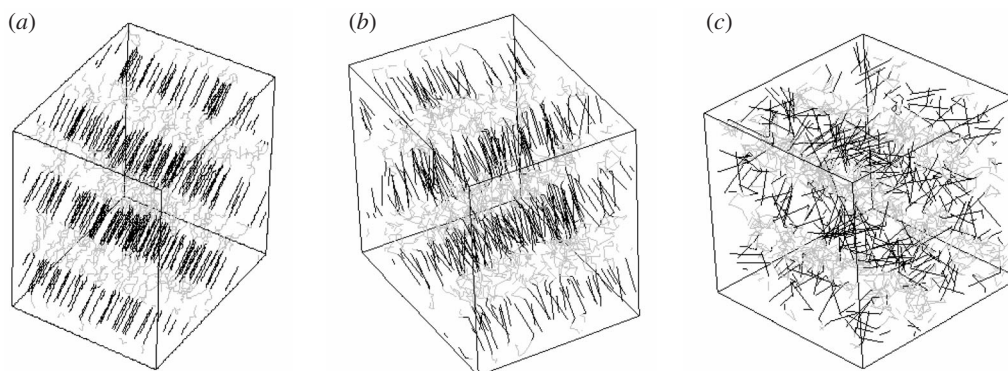


Figure 1. Snapshots of a rod-coil block A_7B_7 copolymer system equilibrated at (a) $T = 0.3$, (b) $T = 0.7$ and (c) $T = 0.9$. For clarity, only one in ten copolymers is shown.

(7 in the coil and 7 in the rod) giving a sample size of 42 000 particles. Simulations of a pure-rods system were carried out under identical conditions, with a total of 6000 rods (again, 42 000 particles). Although pressure scaling already reduces the effects of the periodic box dimensions on the structures formed, additional runs with larger systems are needed to ascertain and minimize these effects. Few runs with a larger simulation box will be carried out in the future.

3. Results and discussion

We started the simulations by placing the diblocks at random in a cubic box, followed by an equilibration at a high temperature with the coil-coil, coil-rod and rod-rod repulsion parameters set to the same value, $a_{CC} = a_{RR} = a_{RC} = 20$.

This resulted in a highly disordered, mixed system, which was then quenched to a temperature of $T = 0.7$, simultaneously increasing the rod-coil repulsion to $a_{RC} = 25$.

Microphase separation set in immediately. At the early stages, the rods formed blobs, which rapidly evolved into elongated stripes. The rods in these stripes were ordered. The stripes then coalesced to form the final lamellar structure depicted in figure 1*b*. Clearly visible is the interdigitation of the rods, as opposed to the formation of bilayer lamellae. The entire process took less than 300 000 time-steps. Notice that symmetric coil-coil block copolymers also form lamellae under the prevailing condition of $\chi N > 10.5$ (Bates & Fredrickson 1990).

The above-described system was further cooled and heated in the temperature range of $0.1 < T < 4.0$, to see what other structures would arise. At the low temperature of $T = 0.3$, a highly ordered system is obtained, as displayed in figure 1*a*. The rods form smooth planes, and they are very well aligned, as in a smectic A phase. Mean square displacements and the radial distribution function reveal that the rods are in a two-dimensional liquid-like state. Lowering the temperature even further resulted in a crystal phase. The smectic C phase predicted (Matsen & Barrett 1998) for high values of χN (remember that lowering the temperature at constant Δa increases χ) has not been observed. At the higher temperature of $T = 0.9$ (see figure 1*c*), the rods and coils are still microphase separated, but the orientational ordering of the rods has largely been lost. Similar smectic to isotropic transitions,

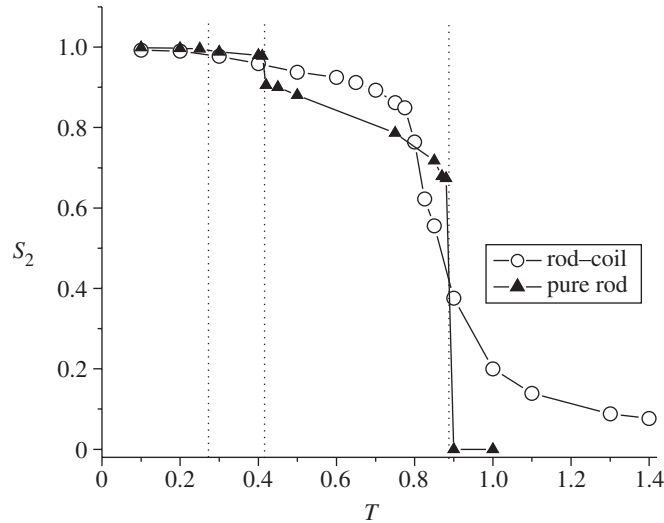


Figure 2. The orientational order parameter S_2 as a function of temperature for an A_7B_7 rod-coil and an A_7 pure-rod system. The dotted lines indicate phase transitions of the pure-rod system.

omitting the nematic, have been reported by a number of authors (Affouard *et al.* 1996; Duchs & Sullivan 2000; van Duijneveldt *et al.* 2000). We will discuss these structures in more detail below.

A quantitative way of looking at these phases is to calculate the matrix

$$\mathbf{Q} = \frac{1}{2}(3\langle \hat{\mathbf{u}}_i \hat{\mathbf{u}}_i \rangle - \mathbf{1}), \quad (3.1)$$

where $\hat{\mathbf{u}}_i$ is the unit vector parallel to the i th rod. The order parameter S_2 is the largest (positive) eigenvalue of this matrix; the corresponding eigenvector $\hat{\mathbf{n}}$ is called the director, as it points in the average direction of the rods. Order is measured here as the width of the distribution of $\hat{\mathbf{u}}_i$ around $\hat{\mathbf{n}}$, and runs from zero (isotropic) to one (parallel rods). A plot of S_2 for the rod-coil copolymer as a function of temperature is shown in figure 2. At low temperatures the order is nearly one. As temperature increases, a gradual decrease is observed. Beyond $T \approx 0.8$ a rapid decay sets in, reaching 0.2 at $T \approx 1.0$. A jump in S_2 , characteristic of a phase transition, is not observed. To rule out the possibility of hysteresis, we have heated and cooled the system through this temperature range, obtaining exactly the same curve in both instances. At higher temperatures the order parameter very slowly decays to zero.

These results are in sharp contrast to those of a pure system of rods. The latter also shows a gradual decrease of S_2 with increasing temperature, but there are also a number of marked jumps: at $T = 0.28$ a crystal to smectic A, at 0.42 a smectic to nematic, and at 0.89 a nematic to isotropic. Note that these liquid-crystalline phases were not observed with rods of less than seven particles, because of their low length-to-width ratio.

Up to $T \approx 0.4$, the S_2 of the pure-rod and rod-coil systems are in quantitative agreement. But whereas the smectic gives way to a nematic in the pure-rod system, the rods in the microphase-separated rod-coil system remain restrained to layers. The propensity of rods to align at these temperatures then forces the system to form a pseudo-smectic phase, with a higher S_2 than the pure-rod system. This pseudo-smectic phase gradually collapses in a temperature range surrounding the clearing

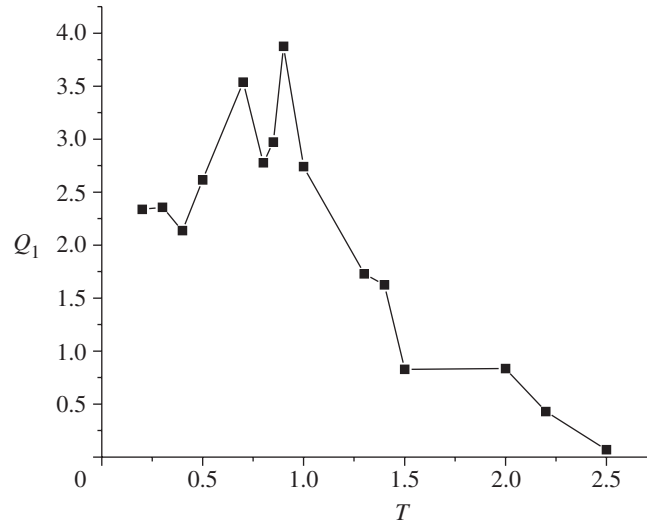


Figure 3. The structural order parameter Q_1 (see the text for its relation to the structure factors) versus temperature.

temperature of the pure-rod system. But because the system is still microphase separated, with the rod layers having a finite width, a small alignment order remains. Of course, the distribution of the angles $\alpha_i = \arccos(\hat{\mathbf{u}}_i \cdot \hat{\mathbf{n}})$ between rods and director flattens as the temperature rises.

The microphase separation process was further investigated by calculating the structure factors

$$S_{\mathbf{R}}(\mathbf{k}) = \frac{1}{N_{\mathbf{R}}} \left\langle \left\{ \left[\sum_{i=1}^{N_{\mathbf{R}}} \sin(\mathbf{k} \cdot \mathbf{r}_i) \right]^2 + \left[\sum_{i=1}^{N_{\mathbf{R}}} \cos(\mathbf{k} \cdot \mathbf{r}_i) \right]^2 \right\} \right\rangle, \quad (3.2)$$

where the sums run over all $N_{\mathbf{R}}$ rod particles. To condense the information contained herein, we have calculated the three eigenvalues of the matrix of second moments of $S_{\mathbf{R}}(\mathbf{k})$, and sorted them by value, $\lambda_1 \leq \lambda_2 \leq \lambda_3$. Symmetry breakdown accompanying the order-disorder transition temperature (ODT) can then be characterized by two invariants (Banaszak & Clarke 1999): $Q_1 = (\lambda_2 + \lambda_3)/\lambda_1 - 2$ and $Q_2 = (\lambda_3 - \lambda_2)/\lambda_1$. The latter remained close to zero at all temperatures, as expected for isotropic and lamellar structures. On the other hand, Q_1 varied with temperature, as can be seen in figure 3. At high temperatures its value is zero and the system is completely isotropic. Only below $T \approx 2.3$ is ordering (lamellar) observed.

These order parameters help us understand the phase diagram of rod-coil diblock copolymers. At temperatures between the ODT and the clearing point (the liquid-crystalline ordering temperature), the rods are collected into layers because of microphase separation, but entropy is not yet sufficiently strong to align the rods. Near the clearing point the rods align within the existing layers; the nematic phase is therefore suppressed and a pseudo-smectic phase is formed. This is a smooth transition, as evidenced by the gradual increase in the orientational order parameter with decreasing temperature. Microphase separation even enhances the ordering process with respect to the pure-rod system.

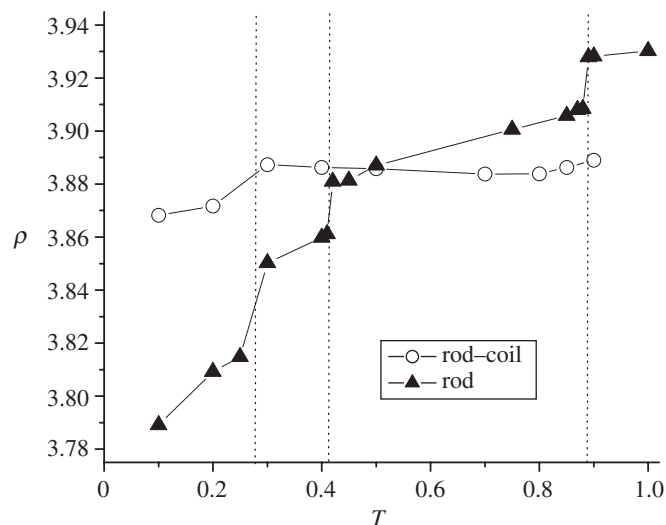


Figure 4. Temperature dependence of the number density, for the rod-coil and the pure-rod system. The dotted lines indicate phase transitions of the pure-rod system.

A curious aspect we have noticed is the variation of number density ρ with temperature, as displayed in figure 4 for the rod-coil system and for a pure-rod system. For the copolymer, the density is almost constant over a wide range of temperatures. At $T \approx 0.2$ the density drops, heralding the onset of crystallization. This onset is more obvious for the pure-rod system, whose density makes a jump at every phase transition. The peculiarity here is that the density increases with increasing temperature, a property it shares with water between 0 and 4 °C. We attribute this effect to the softness of the potential, which has been reported before to give rise to anomalous expansion (Jagla 1999; Stillinger & Weber 1978).

4. Conclusion

We have presented for the first time results for mesoscale simulations of the liquid-crystalline behaviour of both pure-rod fluids and rod-coil copolymers using the dissipative particle dynamics. In addition to its rapid equilibration, DPD with its ultra-soft potential has proven to be a valuable tool for exploring ordering phenomena in complex fluid systems.

For a symmetric rod-coil fluid the effective value of χ was chosen such that the microphase ODT occurred at a temperature well above the mesophase liquid-crystalline (LC) transitions. The significant differences between the LC ordering behaviour of the rod-coil and pure-rod fluids can be rationalized in terms of the imposed lamella structure below the ODT. The nature of the interplay between microphase separation and LC ordering is likely to change significantly for smaller values of χ or for different relative compositions of the rod and coil components of the copolymer. Further simulations, varying among others the repulsion parameters and the rod-to-coil fraction, are currently being pursued.

A.A. thanks the British Council in Saudi Arabia for supporting his stay at UMIST and acknowledges the continuous support of the KFUPM. W.K.d.O. acknowledges the support of the

Training and Mobility in Research Programme of the European Commission under contract no. ERBFMRXCT980176.

References

- Affouard, F., Kroger, M. & Hess, S. 1996 *Phys. Rev. E* **54**, 5178.
- Allen, M. P. & Tildesley, D. J. 1987 *Computer simulation of liquids*. Oxford: Clarendon.
- Banaszak, M. & Clarke, J. 1999 *Phys. Rev. E* **60**, 5753.
- Bates, F. S. & Fredrickson, G. H. 1990 *A. Rev. Phys. Chem.* **41**, 525.
- Chen, J. T., Thomas, E. L., Ober, C. K. & Mao, G. 1996 *Science* **273**, 343.
- Ciccotti, G., Ferrario, M. & Ryckaert, J. P. 1982 *Molec. Phys.* **47**, 1253.
- den Otter, W. K. & Clarke, J. H. R. 2001 *Int. J. Mod. Phys. C* **53**, 426.
- den Otter, W. K. & Clarke, J. H. R. 2004 In *Simulation methods for polymers* (ed. M. Kotelyanskii & D. N. Theodorou). New York: Marcel Dekker.
- Duchs, D. & Sullivan, D. 2000 *J. Phys. Condens. Matter* **14**, 12189.
- Groot, R. D. & Madden, T. J. 1998 *J. Chem. Phys.* **108**, 8713.
- Groot, R. D. & Warren, P. B. 1997 *J. Chem. Phys.* **107**, 4423.
- Jagla, E. 1999 *J. Chem. Phys.* **111**, 8980.
- Jenekhe, S. & Chen, X. 1998 *Science* **279**, 1903.
- Jenekhe, S. & Chen, X. 1999 *Science* **283**, 372.
- Kelker, H. & Hatz, R. 1980 *Handbook of liquid crystals*. Wiley.
- Lee, M., Cho, B. & Zin, W. 2001 *Chem. Rev.* **101**, 3869.
- McBride, C., Vega, C. & MacDowell, L. 2001 *Phys. Rev. E* **64**, 011703.
- Matsen, M. W. & Barrett, C. 1998 *J. Chem. Phys.* **109**, 4108.
- Nicklas, K., Bopp, P. & Brickmann, J. 1994 *J. Chem. Phys.* **101**, 3157.
- Onsager, L. 1949 *Ann. NY Acad. Sci.* **51**, 627.
- Reenders, M. & ten Brinke, G. 2002 *Macromolecules* **35**, 3266.
- Semenov, A. N. 1991 *Mol. Cryst. Liq. Cryst.* **209**, 191.
- Semenov, A. N. & Vasilenko, S. V. 1986 *Sov. Phys. JETP* **63**, 70.
- Stillinger, F. H. & Weber, T. A. 1978 *J. Chem. Phys.* **68**, 3837.
- van Duijneveldt, J., Gil-Vellegas, A., Jackson, G. & Allen, M. P. 2000 *J. Chem. Phys.* **112**, 9092.